

# Study of the thermal behavior of Al(III) and In(III)-diclofenac complexes in solid state

Marcelo Kobelnik · Douglas Lopes Cassimiro ·  
Adélia Emilia de Almeida · Clóvis Augusto Ribeiro ·  
Marisa Spirandeli Crespi

ESTAC2010 Conference Special Issue  
© Akadémiai Kiadó, Budapest, Hungary 2011

**Abstract** The Al and In-diclofenac compounds were prepared. Thermogravimetry (TG) and X-ray diffraction powder patterns were used to characterize these compounds. Details concerning the dehydration and thermal decomposition as well as data of kinetic parameters have been described here. The kinetic studies of these stages were evaluated from several heating rates with mass sample of 2 and 5 mg in open crucibles under nitrogen atmosphere. The results of the present study improve the knowledge on these compounds including their dehydration and thermal stability. The obtained data leads to a dependence on the sample mass, which results in two kinetic behavior patterns.

**Keywords** Diclofenac · Dehydration · Thermal decomposition · Kinetic parameters

## Introduction

The present article is an extension of previous studies [1–3], and it is a part of our research on the thermal behavior interaction among the diclofenac and metal ions. The diclofenac (2-[2,6-dichlorophenylamino]phenylacetate), as it is commonly known, is a useful non-steroidal anti-inflammatory drug [4] for painful diseases of rheumatic and non-rheumatic origin. It is also a good ligand and can be coordinated with several metal ions [5–7]. Thus, we report here the preparation and thermal behavior of solid compounds of aluminum and indium with diclofenac, of general formula  $ML_3 \cdot nH_2O$  (where  $M = Al$  or  $In$ ,  $L$  is diclofenac and  $n = 1$ ). These compounds were investigated by X-ray diffraction powder patterns and TG-DTG. Additionally, for the purpose of comparison this study was carried out with two mass samples, in order to evaluate the effect on the kinetic behavior during thermal decomposition. Thus, the activation energy ( $E_a/kJ mol^{-1}$ ) data were obtained applying the method proposed by Capela and Ribeiro [8, 9].

---

M. Kobelnik  
Centro Universitário do Norte Paulista—UNORP,  
São José do Rio Preto, SP, Brazil

M. Kobelnik  
Instituto de Biociências, Letras e Ciências Exatas,  
São Paulo State University, São José do Rio Preto, SP, Brazil

D. L. Cassimiro · A. E. de Almeida · C. A. Ribeiro ·  
M. S. Crespi  
Instituto de Química, São Paulo State University,  
C.P. 355, Araraquara, SP 14800-900, Brazil

A. E. de Almeida (✉)  
Faculdade de Ciências Farmacêuticas,  
São Paulo State University, São Paulo, SP, Brazil  
e-mail: almeidaa@fcfar.unesp.br

## Experimental

The aluminum and indium-(Diclof)<sub>3</sub> compounds were prepared by the stoichiometric addition of Al and In(II) nitrate on potassium diclofenac salt, both in water solutions. The obtained precipitate was filtered, washed with distilled water, dried at room temperature, and stored in a desiccator over anhydrous calcium chloride until constant weight.

TG/DTG curves were obtained from a SDT 2960 modulus, from TA Instruments. The stoichiometry was obtained by TG analysis using sample sizes of around 5 mg in an  $\alpha$ -alumina crucible and heating rates of  $20\text{ }^\circ\text{C min}^{-1}$

under synthetic air atmosphere ( $100 \text{ mL min}^{-1}$ ). Kinetic evaluation of the steps of the thermal decomposition were obtained using a sample mass around of 2.0 and 5.0 mg with heating rates of 5, 10, and  $20 \text{ }^\circ\text{C min}^{-1}$  under nitrogen atmosphere ( $100 \text{ mL min}^{-1}$ ) from 30 to  $400 \text{ }^\circ\text{C}$  in an alumina crucible.

The X-ray diffraction patterns were obtained from a Siemens D-500 X-ray diffractometer using  $\text{CuK}\alpha$  radiation ( $\lambda = 1.54 \text{ \AA}$ ) and settings of 40 kV and 30 mA.

### Kinetic methodology

Kinetic analysis under non-isothermal conditions is used to consider the integral kinetic equation, defined by

$$\beta = \frac{AE}{Rg(\alpha)} \int_{E/RT}^{\infty} \frac{\exp(-z)}{Z^2} dz \quad (1)$$

where  $\beta = dT/dt$  is a constant heating rate ( $T$  is the temperature and  $t$  is the time),  $g(\alpha)$  the integral form of the reaction model as function of the extent of reaction  $\alpha$ ,  $A$  the pre-exponential factor,  $E$  the activation energy, and  $R$  is the gas constant.

Kinetic parameters are obtained by fitting Eq. 1 to experimental data. As a consequence, the evaluation of the integral on the right side of the Eq. 1 is required, known as temperature integral. A difficulty results from the fact that this integral does not have an exact analytical solution. Thus, it is convenient to approximate the integral of temperature for some function that yields suitable estimates to these kinetic parameters.

In this study, the kinetic parameters are obtained using an isoconversional method on approximation to the temperature integral based on the convergent of a Jacobi fraction, proposed by Capela et al. [9]. This approximation is a rational function, given by the following equation:

$$\int_x^{\infty} \frac{\exp(-z)}{z^2} dz = \frac{\exp(-x)}{x} \frac{x^3 + 14x^2 + 46x + 24}{x^4 + 16x^3 + 72x^2 + 96x + 24} \quad (2)$$

A characteristic experimental curve presents the conversional fraction,  $\alpha$ , as a function of the temperature for a given heating rate,  $\beta$ . For each fixed value of  $\alpha$  there are corresponding values  $T_\alpha$  for temperature, values  $E_\alpha$  for activation energy and values  $A_\alpha$  for pre-exponential factor.

Replacing the integral in Eq. 1 by the approximation given in Eq. 2 the following expression for heating rate  $\beta$  as function of the  $x_\alpha = 10^3/RT_\alpha$  is obtained:

$$\beta = \frac{\exp(B_\alpha - E_\alpha z_\alpha)}{x_\alpha} \frac{E_\alpha^3 z_\alpha^3 + 14E_\alpha^2 z_\alpha^2 + 46E_\alpha z_\alpha + 24}{E_\alpha^4 z_\alpha^4 + 16E_\alpha^3 z_\alpha^3 + 72E_\alpha^2 z_\alpha^2 + 96E_\alpha z_\alpha + 24} \quad (3)$$

where the activation energy is in kJ/mol and the parameter  $B_\alpha$  is defined as:

$$B_\alpha = \ln\left(\frac{10^3 A_\alpha}{Rg(\alpha)}\right) \quad (4)$$

The estimates of the  $E_\alpha$  and  $B_\alpha$  can be obtained by the non-linear fitting of the Eq. 3 to the  $\beta$  values as a function of  $x_\alpha$ .

Once the  $g(\alpha)$  function has been determined for each conversional fraction  $\alpha$ , the estimation of the Arrhenius pre-exponential factor can be obtained from Eq. 4 and is given by the following equation:

$$\hat{A}_\alpha = \frac{R}{10^3} \exp(\hat{B}_\alpha) g(\alpha) \quad (5)$$

### Results and discussion

Simultaneous TG-DTG curves of  $\text{Al}(\text{Diclof})_3 \cdot \text{H}_2\text{O}$  and  $\text{In}(\text{Diclof})_3 \cdot \text{H}_2\text{O}$  are shown in Figs. 1 and 2, respectively.

For the aluminum compound, the first mass loss occurred only between 30 and  $110 \text{ }^\circ\text{C}$  (TG) due to dehydration, with a loss of 1.76%, corresponding to the endothermic peak ( $91 \text{ }^\circ\text{C}$ ) in the DSC curve. After dehydration, between 191 and  $638 \text{ }^\circ\text{C}$ , the thermal decomposition occurs in two stages of mass losses. The first stage, from 191 to  $360 \text{ }^\circ\text{C}$ , is due to the initial decomposition of this compound and occurs in an overlapping reaction, corresponding to the endothermic peak in the DSC curve, both at 300 and  $335 \text{ }^\circ\text{C}$ , with a loss of 74.75%. The second stage of the thermal decomposition of this compound occurs in two stages between 477 and  $638 \text{ }^\circ\text{C}$  and corresponding to the exotherm between 510 and  $588 \text{ }^\circ\text{C}$ , with a loss of 18.48%. The total mass loss up to  $638 \text{ }^\circ\text{C}$  is in agreement with the formation of  $\text{Al}_2\text{O}_3$ , as a final residue. Furthermore, analyzing the DSC curve after the dehydration process, we can see three peaks (one endothermic and two

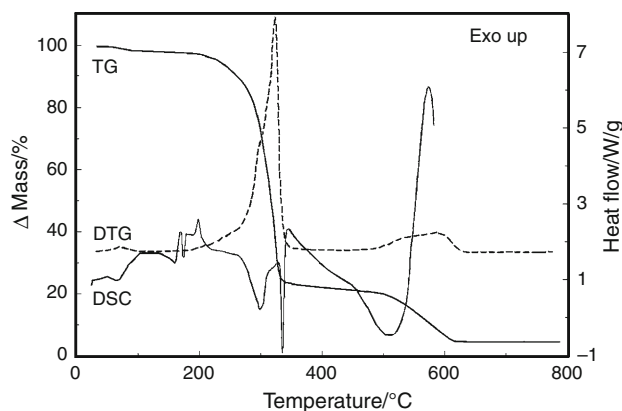


**Fig. 1** TG/DTG and DSC curves of the  $\text{Al}(\text{Diclof})_3 \cdot \text{H}_2\text{O}$  compound in synthetic air and heating rate of  $20 \text{ }^\circ\text{C min}^{-1}$

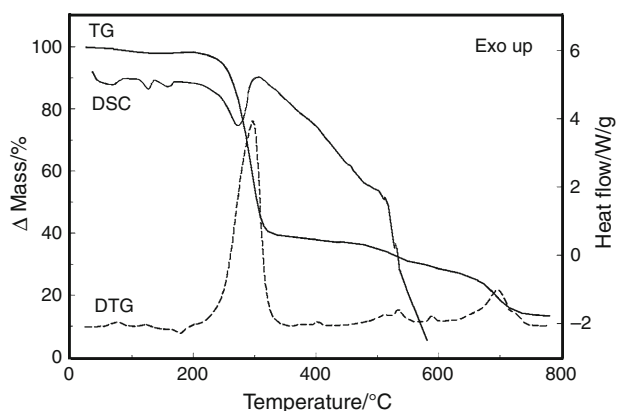


**Fig. 2** TG/DTG and DSC curves of the  $\text{In}(\text{Diclof})_3 \text{H}_2\text{O}$  compound in synthetic air and heating rate of  $20\text{ }^\circ\text{C min}^{-1}$

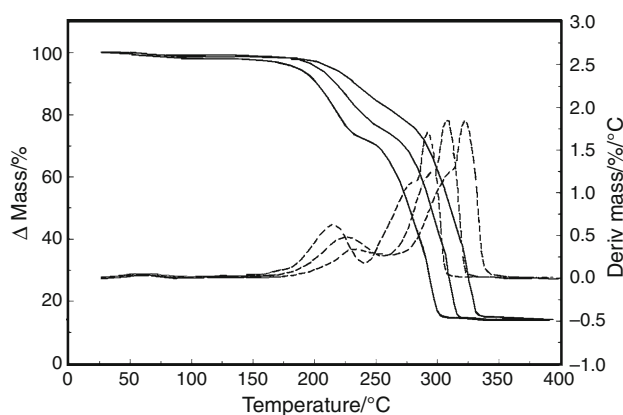


**Fig. 3** TG/DTG curves of  $\text{Al}(\text{Diclof})_3$  compound in nitrogen atmosphere at heating rate of  $5, 10, \text{ and } 20\text{ }^\circ\text{C min}^{-1}$ , in aluminum crucible and sample mass of  $2\text{ mg}$

exothermic) between  $134$  and  $209\text{ }^\circ\text{C}$ , which were attributed to the transition phase.

For the indium compound, the first mass loss is due to the dehydration stage and occurs between  $35$  and  $100\text{ }^\circ\text{C}$  and has loss of  $1.80\%$ , which corresponds to the endothermic peak at  $67\text{ }^\circ\text{C}$  (DSC). After dehydration, the thermal decomposition occurs between  $216$  and  $750\text{ }^\circ\text{C}$  in two stages of mass loss. The first stage, from  $216$  to  $335\text{ }^\circ\text{C}$  ( $58.09\%$ ), is attributed to the initial decomposition of this compound and corresponds to the endothermic event ( $275\text{ }^\circ\text{C}$ ), as seen in the DSC curve. The second decomposition stage occurs with overlapping reactions and corresponds to a mass loss of  $26.68\%$  and, thus as aluminum compound, a significant exothermic or endothermic event was not observed. Calculations based on the total mass loss up to  $750\text{ }^\circ\text{C}$  are in agreement with the formation of  $\text{In}_2\text{O}_3$ , as a final residue. As well as the aluminum compound, two endothermic events can be seen between  $110$  and  $170\text{ }^\circ\text{C}$ , which are attributed to the transition phase.

Figures 3, 4, 5, and 6 show the TG/DTG curves for  $\text{Al}(\text{Diclof})_3$  and  $\text{In}(\text{Diclof})_3$  compounds in a nitrogen

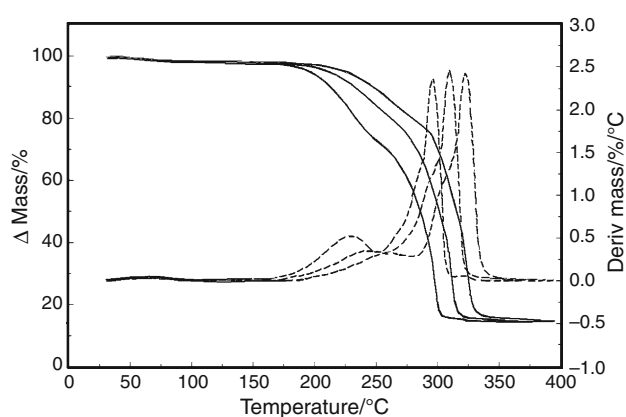


**Fig. 4** TG TG/DTG curves of  $\text{Al}(\text{Diclof})_3$  compound in nitrogen atmosphere at heating rate of  $5, 10, \text{ and } 20\text{ }^\circ\text{C min}^{-1}$ , in aluminum crucible and sample mass of  $5\text{ mg}$

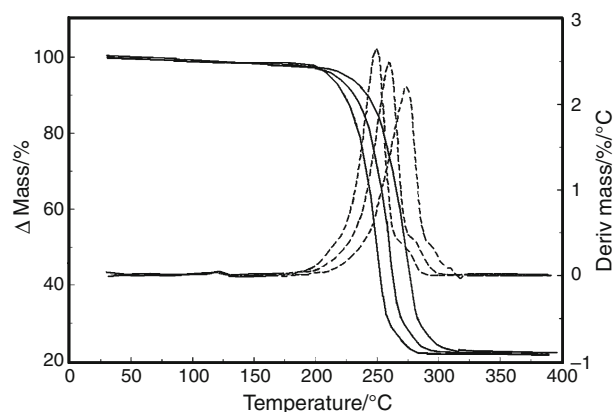


**Fig. 5** TG TG/DTG curves of  $\text{In}(\text{Diclof})_3$  compound in nitrogen atmosphere at heating rate of  $5, 10, \text{ and } 20\text{ }^\circ\text{C min}^{-1}$ , in aluminum crucible and sample mass of  $2\text{ mg}$

atmosphere with a sample mass of  $2$  and  $5\text{ mg}$ , respectively, which were used for the kinetic study. For the aluminum compound, the stage of dehydration does not occur similarly to that of synthetic air. This disagreement most probably is due to dehydration of these compounds in the desiccator over anhydrous calcium chloride, because the TG curves were obtained 12 months after the DSC and TG-DTG curves (Fig. 1). Besides, due to the decrease of the water loss and also because of an imperfect DTG curve it becomes much more difficult to establish the range of the values for kinetic study. The thermal decomposition is very different from synthetic air. The mass losses occur in two stages, between  $170$  to  $278\text{ }^\circ\text{C}$  (first stage) and  $237$  to  $335\text{ }^\circ\text{C}$  (second stage), with losses around  $22.50$  and  $62.00\%$ , respectively.

For the indium compound, for the dehydration stage the same disagreement occurs, which is due to the extended time in the desiccator. The thermal decomposition is also very different from synthetic air, and the mass losses occur

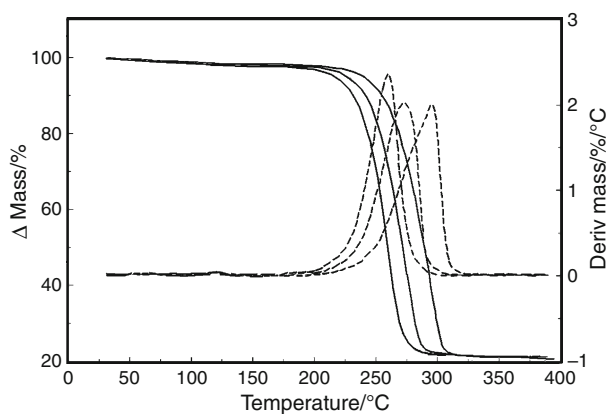


**Fig. 6** TG TG/DTG curves of In(Diclof)<sub>3</sub> compound in nitrogen atmosphere at heating rate of 5, 10, and 20 °C min<sup>-1</sup>, in aluminum crucible and sample mass of 5 mg

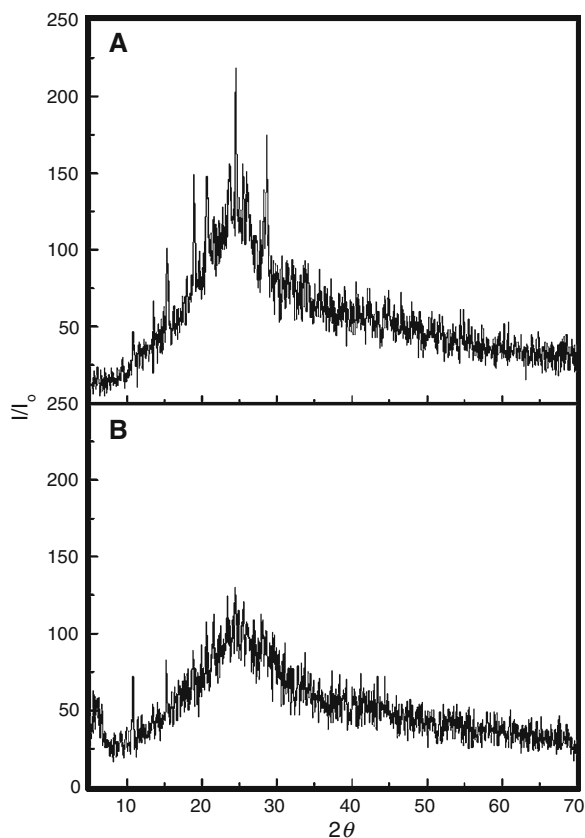


**Fig. 7** Characteristic parts of X-ray diffraction pattern: Al(Diclof)<sub>3</sub> (a) and In(Diclof)<sub>3</sub> (b)

in only one stage, between 205 and 309 °C, both the sample masses showing losses of around 76%. For the mass of 2 mg (DTG curve) we can be seen the presence of overlapping reactions at the end of the decomposition reaction can be seen and, therefore, this step was not considered to determine the kinetic parameters.

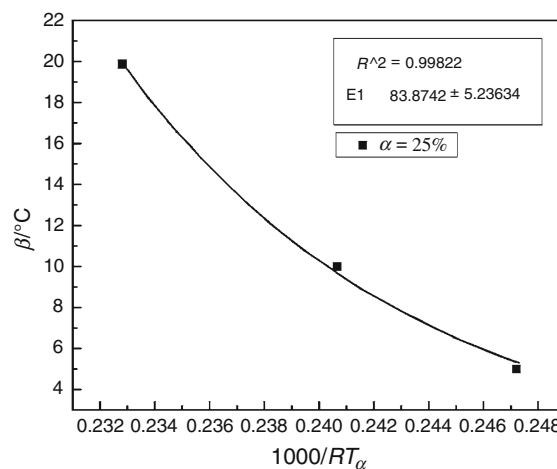


**Fig. 8** Diagram of dispersion of  $\beta$  versus degree conversion ( $\alpha$ —25%) of the Al(Diclof)<sub>3</sub> compound to first thermal decomposition for 5 mg, with the adjustment functions

**Table 1**  $E_a$  (kJ mol<sup>-1</sup>) and correlation coefficient ( $r$ ) for the thermal decomposition stage

Compound	Sample mass	$E_a^*/\text{kJ mol}^{-1}$	$r^*$
Al(Diclof) <sub>3</sub>	2 mg decomposition stage	144.79 ± 0.11	0.98914
	5 mg decomposition stage	84.41 ± 0.02	0.99231
In(Diclof) <sub>3</sub>	2 mg decomposition stage	127.45 ± 0.03	0.98307
	5 mg decomposition stage	101.81 ± 0.04	0.99525

\* Average

The X-ray powder patterns of these compounds are shown in Fig. 7. In Fig. 7a, it is observed the presence of some characteristic lines for the aluminum compound can be observed, which indicate that this compound has a crystalline structure. However, for the indium compound, shown in Fig. 7b, the diffraction lines were not observed, which demonstrates that this compound is non-crystalline.

#### Kinetic parameters

The kinetic parameters of these compounds were evaluated from the DTG curves (Figs. 3, 4, 5, and 6, respectively). The activation energy ( $E_a$ ) versus conversion degree ( $\alpha$ ) values for the first decomposition stage of sample masses of 2 and 5 mg are shown in Fig. 9.

Figure 8 shows the calculations for the activation energy and correlation coefficient ( $r$ ) for the decomposition stage for the Al(Diclof)<sub>3</sub> compound with a 5 mg sample. The average values of the activation energy ( $E_a$ ) of the kinetic data of the different experimental adjustments (5–95%) for all steps are shown in Table 1. The resulting correlation coefficient has a good close linear fit ( $r$ ).

The calculated activation energy as a function of conversion degree ( $\alpha$ ) for the decomposition stage is shown in

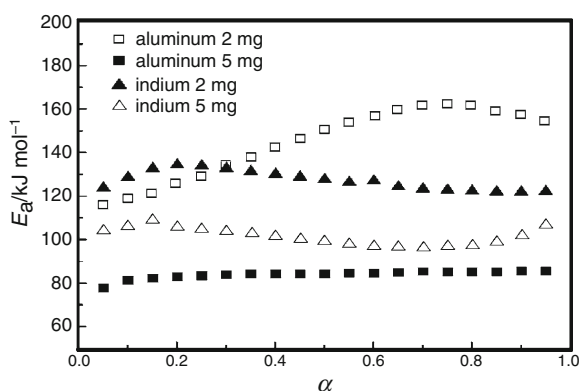


**Fig. 9** The calculated  $E_a/\text{kJ mol}^{-1}$  as a function of  $\alpha$  for the decomposition stage

the Fig. 9. We can see that aluminum compound, with sample mass of 2 mg, without the tendencies of the plots maintain the same contour and run parallel as with the sample mass of 5 mg. This indicates that kinetic decomposition does not occur with the same way for every extension of  $\alpha$ , from both the samples. However, for the indium compound we can see that the plots maintain the same contour, and therefore, indicate that there is the same tendency of thermal decomposition for both the mass samples.

Comparing the results between aluminum and indium compounds, the thermal decomposition of indium suggested that the shape of the conversion degree ( $\alpha$ ) resulted from only one reaction process. However, for the aluminum compound it is clear that the activation energy has a different behavior on all the extent of the conversion degree. Probably, there are the occurrences of a multi-step process in every stage of the thermal decomposition. For both compounds, it is also evident that the apparent activation energy becomes lower with an increasing in the mass of the sample. In a previous study, Kobelnik et al. observed that for  $\text{Zn}(\text{Diclof})_2$  there is an increase in the activation energy for a sample mass of 5 mg in function of conversion degree as numerical values. The obtained results were also attributed to the overlapping reactions [3] in this study.

## Conclusions

The thermal studies carried out in non-isothermal TG in  $\text{N}_2$  and in air, provide an understanding of the behavior during

thermal analysis. Furthermore, the DTG and DSC curves provided information concerning the thermal stability and thermal decomposition of these compounds that had not been reported previously. The X-ray powder diffraction patterns reveal that the aluminum compound has a crystalline structure.

As well as this, the kinetic dependence on the experimental condition, conditioned by contributions of two different mass samples, allows a better evaluation of kinetic parameters. Moreover, the kinetic behavior demonstrates that the increase in sample mass causes a decrease in the activation energy values.

**Acknowledgements** We express our deepest gratitude to CAPES Foundation, Brazil, for financial support, and to IPT—Instituto de Pesquisas Tecnológicas do Estado de São Paulo by TG curves.

## References

1. Kobelnik M, Bernabé GA, Ribeiro CA, Capela JMV, Fertonani FLJ. Decomposition kinetics of iron (III)-diclofenac compound. *J Therm Anal Calorim.* 2009;97:493–6.
2. Kobelnik M, Cassimiro DL, Ribeiro CA, Dias DS, Crespi MS. Preparation of the Ca–diclofenac complex in solid state. Study of the thermal behavior of the dehydration, transition phase and decomposition. *J Therm Anal Calorim.* doi 10.1007/s10973-010-0787-8.
3. Kobelnik M, Quarcioni VA, Ribeiro CA, Capela JMV, Dias DS, Crespi MS. Thermal study in solid state of Zn(II)-diclofenac complex: behavior kinetic of the dehydration, transition phase and thermal decomposition. *J Chin Chem Soc.* 2010;57:384–90.
4. Konstandinidou M, Kourounakis A, Yiangou M, Hadjipetrou L, Kovala-Demertzi D, Hadjidakou S, Demertzis M. Anti-inflammatory properties of diclofenac transition metalloelement complexes. *J Inorg Biochem.* 1998;70:63–9.
5. Kovala-Demertzi D, Hadjidakou SK, Demertzis MA, Deligiannakis Y. Metal ion–drug interactions. Preparation and properties of manganese (II), cobalt (II) and nickel (II) complexes of diclofenac with potentially interesting anti-inflammatory activity: Behavior in the oxidation of 3,5-di-tert-butyl-*o*-catechol. *J Inorg Biochem.* 1998;69:223–9.
6. Bucci R, Magri AD, Magri AL, Napoli A. Spectroscopic characteristics and thermal properties of divalent metal complexes of diclofenac. *Polyhedron.* 2000;19:2515–20.
7. Ihsan MK. Density functional theory assessment of the thermal degradation of diclofenac and its calcium and iron complexes. *J Mol Struct.* 2005;754:61–70.
8. Souza JL, Kobelnik M, Ribeiro CA, Capela JMV. Kinetics study of crystallization of PHB in presence of hydrociacids. *J Therm Anal Calorim.* 2009;97:525–8.
9. Capela JMV, Capela MV, Ribeiro CA. Nonisothermal kinetic parameters estimated using nonlinear regression. *J Math Chem.* 2009;45:769–75.